

Supporting Information

Thermodynamically Self-organized Hole Transport Layer for High-Efficiency Inverted-Planar Perovskite Solar Cells

*Wanjung Kim, Soyeon Kim, Sung Uk Chai, Myung Sun Jung, Jae Keun Nam, Jung-Hyun Kim
* and Jong Hyeok Park **

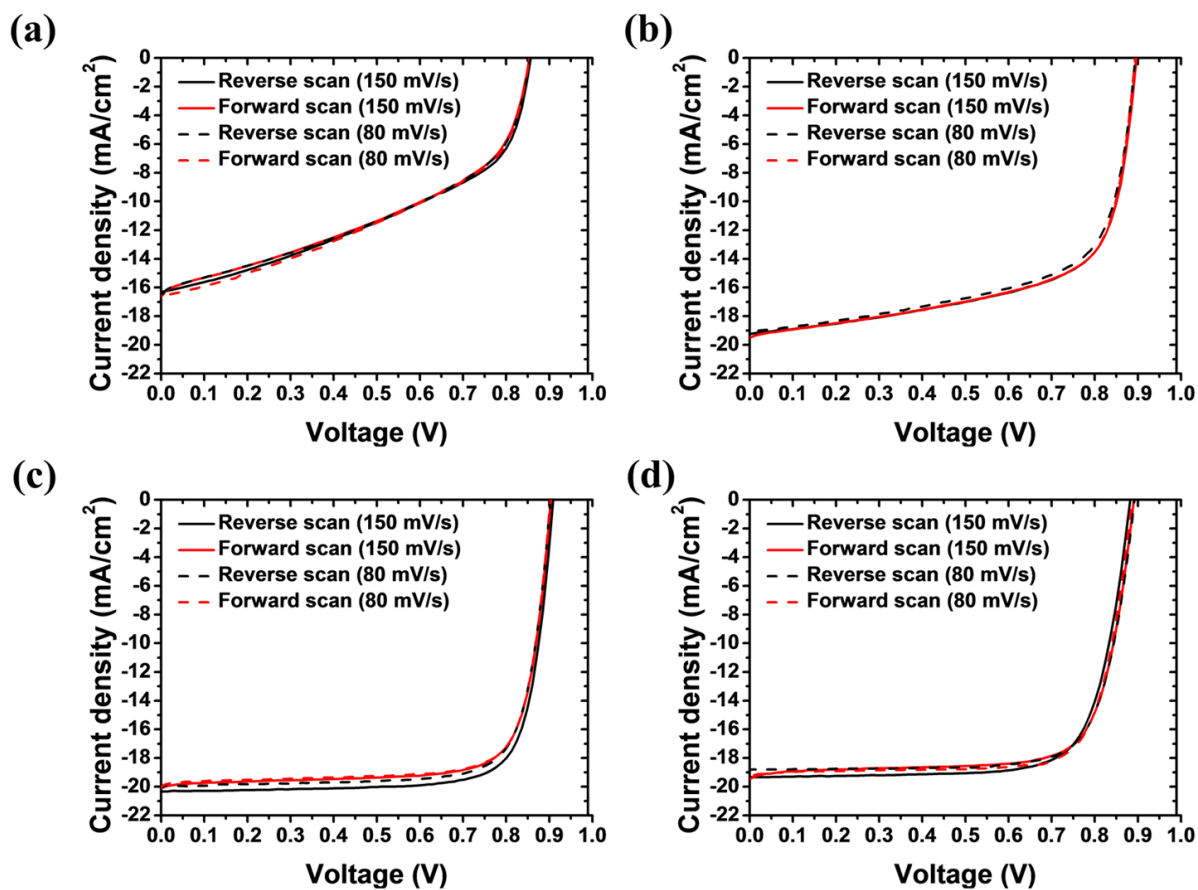


Fig. S1. J - V curves measured by forward (from J_{SC} to V_{OC} , red) and reverse scans (from V_{OC} to J_{SC} , black) of the IP-PSCs containing various PEDOT:PSS films depending on the PSS/PEDOT ratio: (a) PEDOT1:PSS0.5, (b) PEDOT1:PSS2.5, (c) PEDOT1:PSS5.0 and (d) PEDOT1:PSS12.

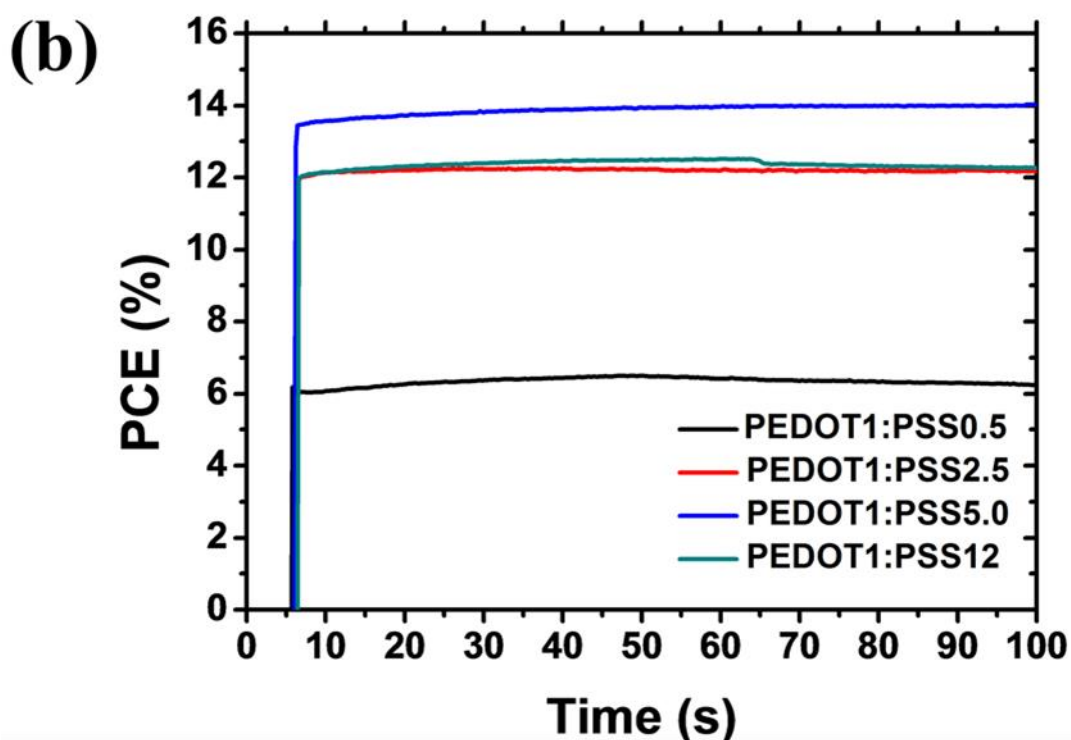
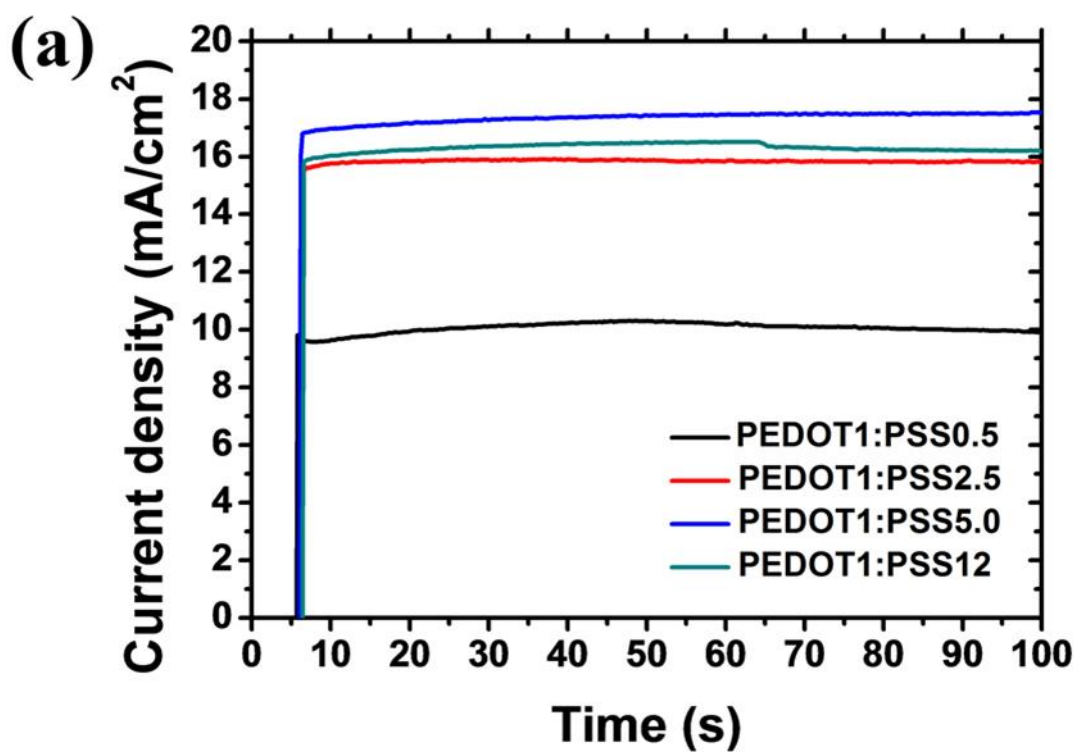


Fig. S2. (a) Photocurrent density and (b) power conversion efficiency as a function of time for the IP-PSC devices containing PEDOT:PSS films with controlled weight ratios. Data were obtained at the maximum voltage, $V_{max}=0.63$ (PEDOT1:PSS0.5), 0.77 (PEDOT1:PSS2.5), 0.8 (PEDOT1:PSS5.0) and 0.76 (PEDOT1:PSS12), without pre-exposure under 1 sun illumination.

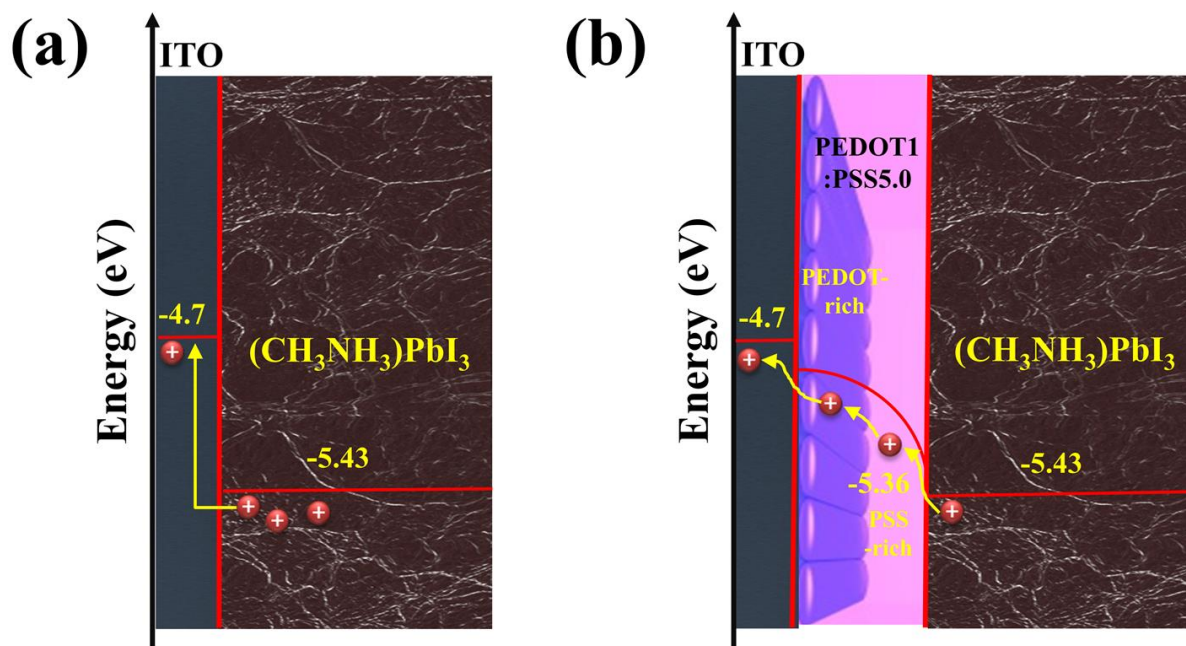


Fig. S3. (a) Schematic of a hole-transport process from perovskite layer to ITO electrode. (b) Schematic of a hole-transport process from perovskite layer to ITO electrode via PEDOT1:PSS5.0 layer.

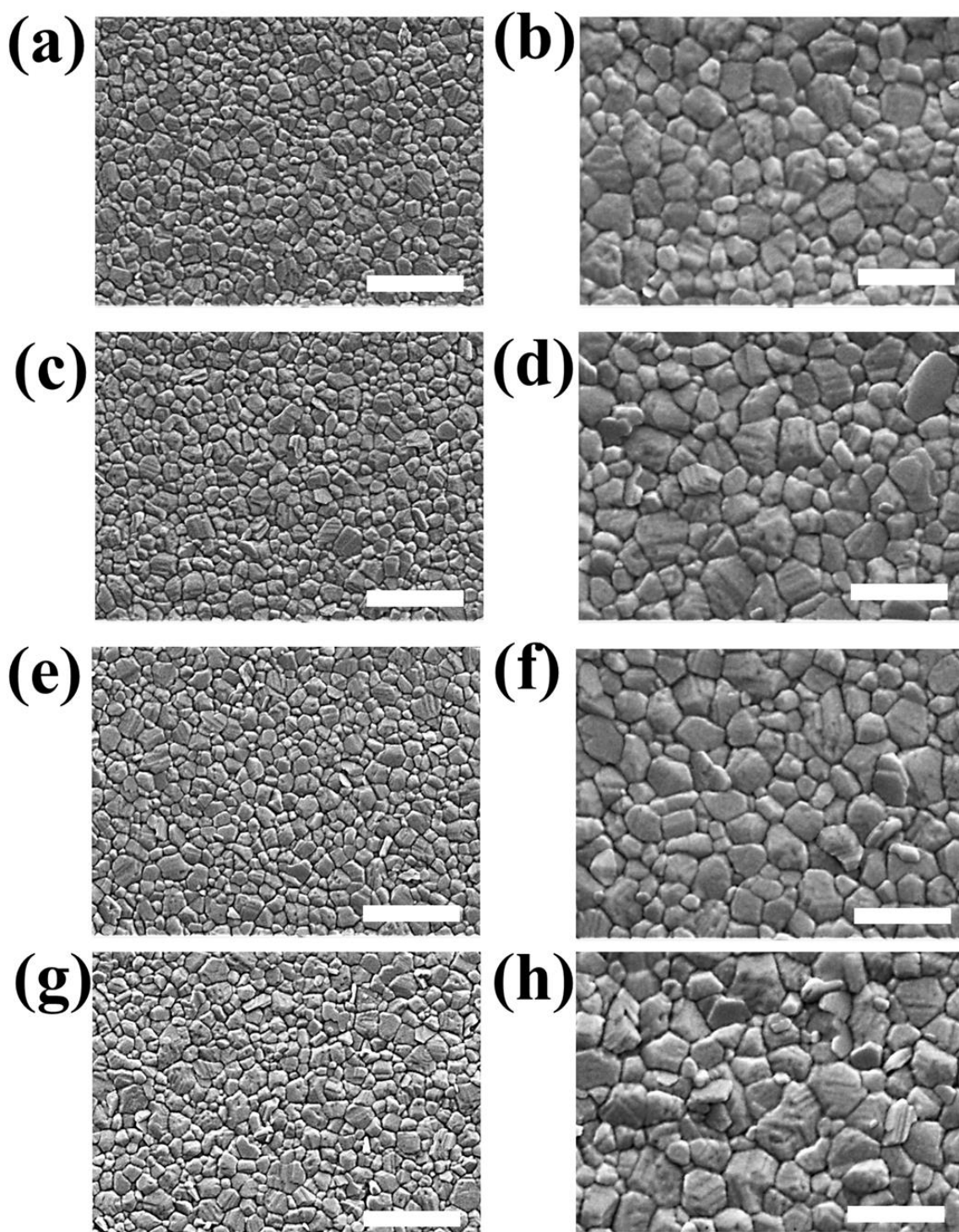


Fig. S4. Top-view SEM image of MAPbI₃ films on the various PEDOT:PSS layers depending on the PSS/PEDOT ratio: (a-b) PEDOT1:PSS0.5, (c-d) PEDOT1:PSS2.5, (e-f) PEDOT1:PSS5.0 and (g-h) PEDOT1:PSS12. Scale bar, 1000 nm (a, c, e, g) and 500 nm (b, d, f, h).

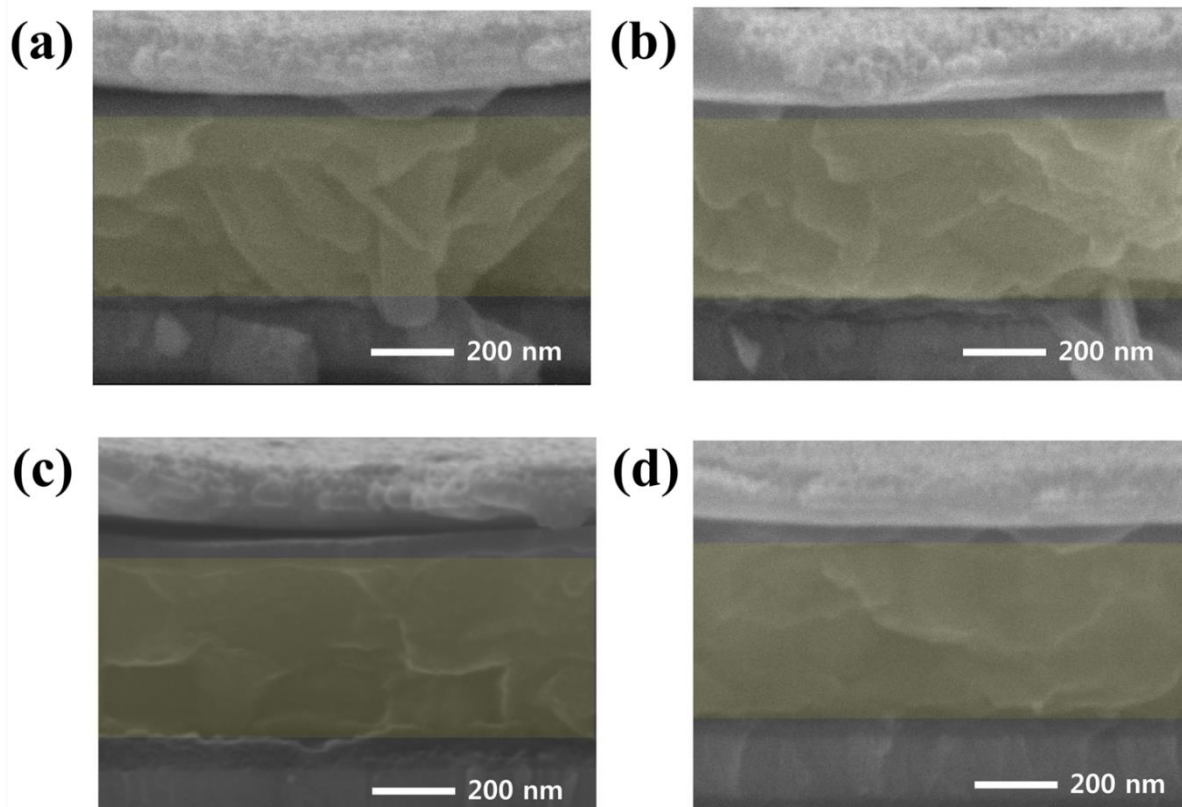


Fig. S5. Cross-sectional SEM images of the MAPbI₃ films on the various PEDOT:PSS layers depending on the PSS/PEDOT ratio: (a) PEDOT1:PSS0.5, (b) PEDOT1:PSS2.5, (c) PEDOT1:PSS5.0 and (d) PEDOT1:PSS12.

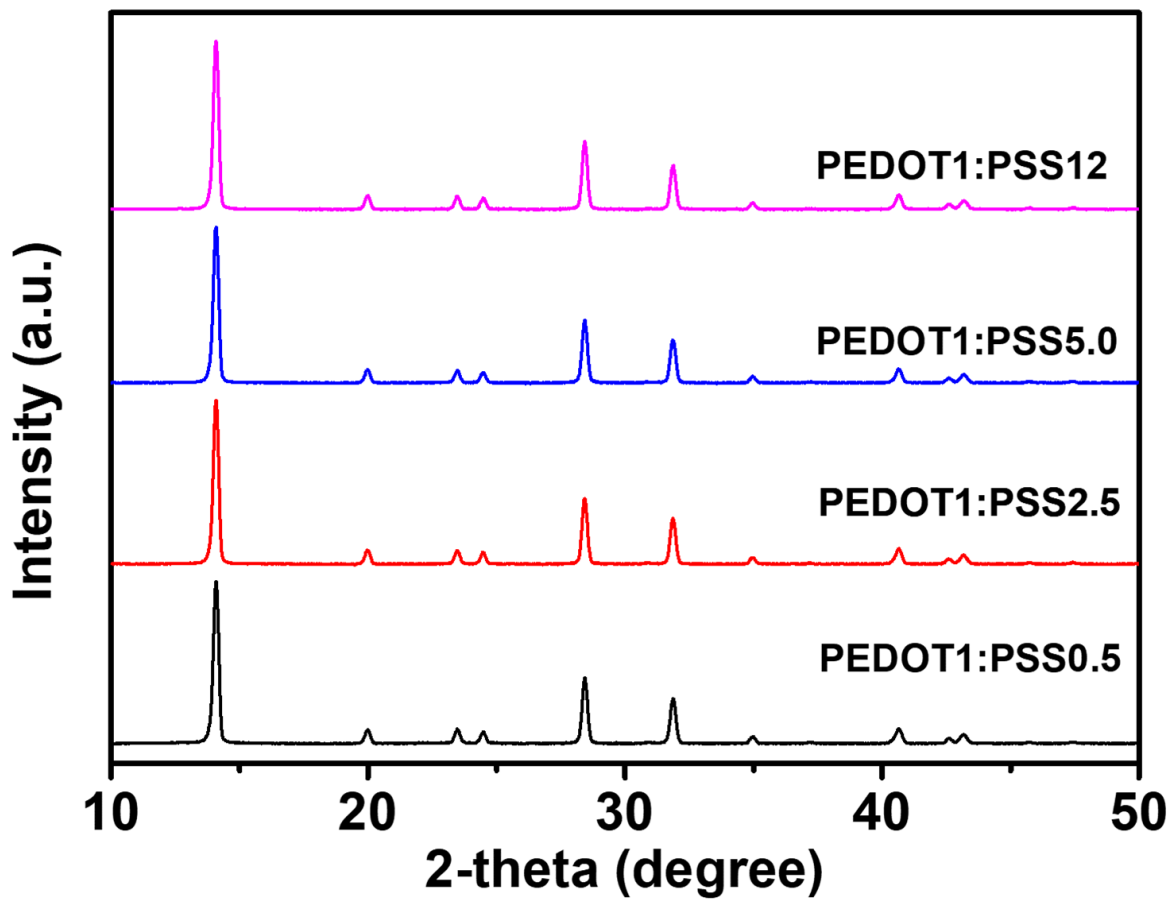


Fig. S6. XRD patterns of MAPbI₃ films on the various PEDOT:PSS layers depending on the PSS/PEDOT ratio

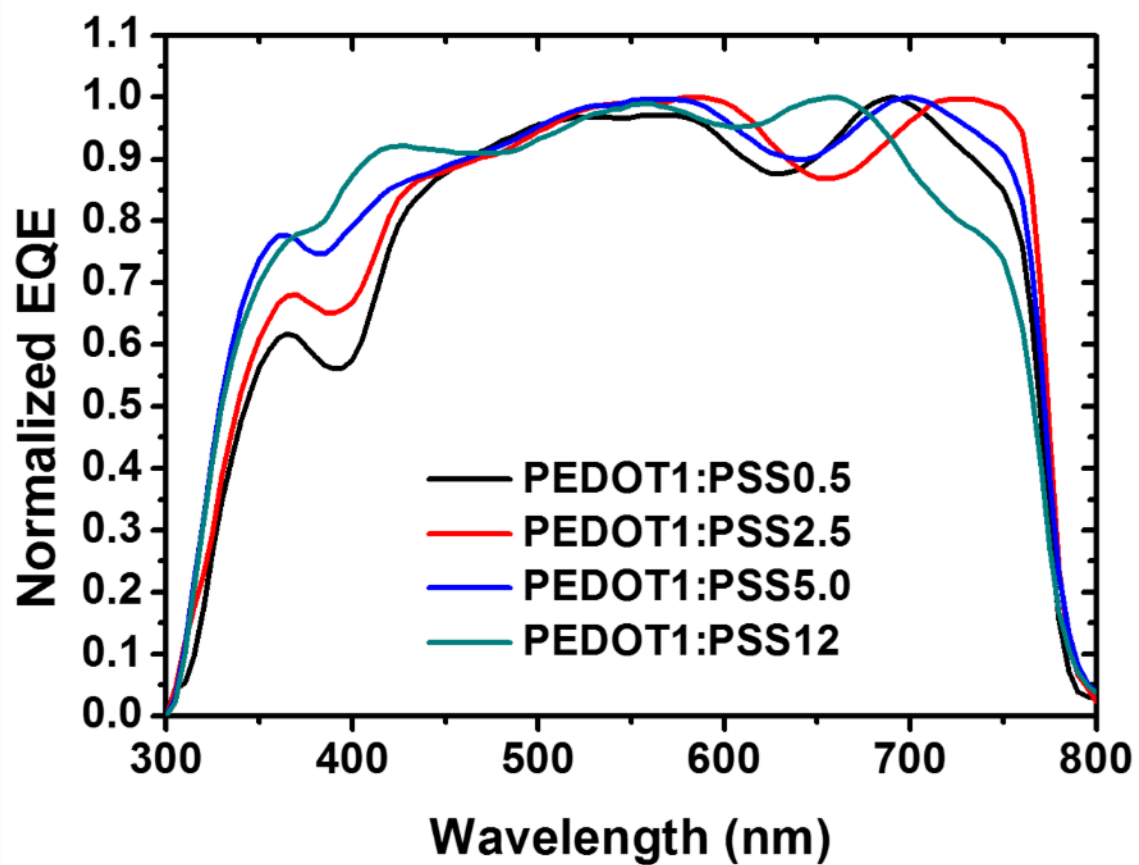


Fig. S7. Normalized EQE spectra of the IP-PSCs containing various PEDOT:PSS layers depending on the PSS/PEDOT ratio.